Substrate Discrimination by the Human GTP Fucose Pyrophosphorylase

Stephen Quirk‡ and Katherine L. Seley*

Department of Chemistry and Biochemistry, University of Maryland, Baltimore County, 1000 Hilltop Circle, Baltimore, Maryland 21250

Received February 25, 2005; Revised Manuscript Received June 3, 2005

ABSTRACT: GTP-L-fucose pyrophosphorylase (GFPP, E. C. 2.7.7.30) catalyzes the reversible condensation of guanosine triphosphate and β-L-fucose-1-phosphate to form the nucleotide−sugar GDP-β-L-fucose. The enzyme functions primarily in the mammalian liver and kidney to salvage free L-fucose during the breakdown of glycolipids and glycoproteins. The mechanism by which this protein discriminates between substrate and nonsubstrate molecules has been elucidated for the first time in this study. The ability of GFPP to form nucleotide−sugars from a series of base-, ribose-, phosphate-, and hexose-modified precursor molecules has revealed that the enzyme active site senses a series of substrate substituents that drive substrate/nonsubstrate discrimination. These substituents alter the ability of the precursor molecule to interact with the enzyme, as measured by either changes in the Michaelis constant, K_m, the binding affinity, K_a, or through changes in enzymatic turnover, k_{cat}. In this work, the combined substrate binding and enzyme analysis has revealed that the nature of the purine base is the major determinant in substrate specificity, followed by the nature of the hexose-1-P, and finally by the ribose moiety. Binding is enthalpy-driven and does not involve proton transfer. For the majority of nucleotide−sugar analogues, binding to GFPP is entropically unfavorable; however, surprisingly, a few of the substrate analogues tested bind to GFPP with a favorable entropic term.

Fucose is a deoxyhexose that is found in nearly all plant and animal species. The monosaccharide plays several important metabolic roles in complex carbohydrates and in glycoproteins (reviewed in ref *1*). Fucosylated oligosaccharides are involved in cell−cell recognition (*2*), selectin-mediated leukocyte−endothelial adhesion (*3*), and mouse embryogenesis (*4*). They form the basis of the Lewis-type blood group antigens (*5*), are involved in the formation of atherosclerosis (*6*), and mediate host−bacterial interactions (*7*). A decrease in the availability of fucose is associated with leukocyte adhesion deficiency type-II disorder (*8*), and fucosylated glycoproteins have been implicated in memory processes (*9*, *10*). Fucose is made available during the synthesis of fucosylated glycolipids, oligosaccharides, and glycoproteins via a sugar nucleotide intermediate, specifically GDP-β-L-fucose. In most organisms, GDP-fucose is formed predominantly by the oxidation−reduction and epimerization of GDP-α-D-mannose (*11*). In mammals, a second pathway exists for the formation of GDP-β-L-fucose. Specifically, a salvage pathway converts the fucose liberated from the metabolism of glycoproteins, glycolipids, and fucose-containing oligosaccharides to fucose-1-phosphate and subsequently to GDP-β-L-fucose. The first reaction is catalyzed by an ubiquitous fucosyl kinase (*12*, *13*). The second reaction is catalyzed by a novel guanosine triphosphate fucose pyrophosphorylase (*14*).

Guanosine triphosphate fucose pyrophosphorylase (GFPP, E. C. 2.7.7.30) catalyzes the formation of GDP-L-fucose from GTP and fucose-1-phosphate according to the following reaction:

$$\text{GTP} + \text{fucose-1-P} \leftrightarrow \text{GDP-L-fucose} + \text{PP}_i$$

The reversible reaction is dependent on a small number of divalent cations, with a preference for magnesium, cobalt, or manganese (*14*). The reaction is unusual in that, of the four canonical nucleoside triphosphates, only guanosine and to a lesser extent inosine can be utilized to form a nucleotide−sugar (*14*). Furthermore, the enzyme does not catalyze the formation of inorganic orthophosphate from the liberated pyrophosphate moiety as a way of energetically driving the reaction in the product formation direction.

Nucleotide−sugar metabolizing enzymes can drive substrate specificity through active-site recognition of three distinct chemical moieties: the base, the ribose species, and the hexose. This implies that the active site of GFPP may be comprised of three distinct regions that are spatially arranged to align the NTP and the hexose-1-P for catalysis. Complex active-site architectures that are linked to unusual enzymatic mechanisms are a hallmark of enzymes that metabolize nucleotide−sugars (*15*−*22*).

This study seeks to further the understanding of the human GFPP enzyme active site as a prelude to continued structure−function studies. The enzyme remains refractory to crystallization, even though it can be purified to homogeneity from native sources or produced recombinantly. In this work, human GFPP substrate discrimination has been dissected with a series of analogues. The use of combined enzymatic and thermodynamic measures has allowed a better understanding of which nucleotide−sugar constituents are important for binding and/or catalysis. The apparent discrimination by

* To whom correspondence should be addressed: Department of Chemistry and Biochemistry, University of Maryland, Baltimore Co., 1000 Hilltop Circle, Chemistry Building, Room 108, Baltimore, MD 21250. Telephone: 410-455-8684. Fax: 410-455-2608. E-mail: kseley@umbc.edu.

‡ Current address: Kimberly-Clark Corp, Roswell, GA.

10.1021/bi0503605 CCC: $30.25
Published on Web 07/19/2005

GFFP for a guanine base implies that the enzyme active site is more restrictive for base recognition than is typical for similar enzymes (*23*).

EXPERIMENTAL PROCEDURES

Construction of a GTP Fucose Pyrophosphorylase Expression Plasmid. Unless otherwise noted all procedures performed in this study were according to Sambrook et al. (*24*), including bacteria plating, agarose gel electrophoresis, and restriction endonuclease digestions. The gene that encodes GTP fucose pyrophosphorylase (GFPP) was isolated from a pool of human liver-specific cDNA (Invitrogen, Inc.) using two primers:

5′-ACACACCATATGGCAGCTGCTAGGGACCCT

and

5′-GTGTGTCTCGAGCTACATCAAACTGCTTTTT-AAAC

The first primer incorporates a flanking *Nde* I restriction site directly upstream from the initiating ATG codon. An *Xho* I restriction site is incorporated into the second primer directly after the stop codon. The primer sequences that correspond to the GFPP coding region were derived from the published DNA sequence (GenBank accession AF017455). PCR reactions using these two primers amplified the entire 1782 bp coding region. Typical PCR reactions were as follows: 94 °C for 5 min, followed by 30 cycles of 94 °C for 1 min, 54 °C for 1 min, and 72 °C for 2 min. After the last cycle, the PCR reaction was held at 72 °C for 10 min. The PCR DNA band was purified using the Wizard PCR DNA cleanup kit (Promega). The insert was digested with *Nde* I and *Xho* I (both from New England Biolabs) and was repurified. Digested GFPP insert was combined in a 10:1 molar excess with *Nde* I/*Xho* I digested pET15b. Ligations were performed with T4 DNA ligase at 14 °C for 12 h. Aliquots of the ligation reaction were used to transform chemically competent DH5α bacteria. Recombinant molecules were verified by DNA sequencing from minipreps. One positive colony was designated as pGSPPe.

Purification of GTP Fucose Pyrophosphorylase. Human GFPP enzyme was purified to homogeneity by growing 3 L of pGFPPe/BL21(DE3) culture (in LB supplemented with 60 μg/mL ampicillin) at 37 °C until an $OD_{595} = 0.6$ was reached. Protein expression was induced by the addition of IPTG to a final concentration of 1 mM, and growth was continued for 5 h. Cells were pelleted by centrifugation at 11000*g* for 15 min. The collected cell paste was frozen at −20 °C for at least 2 h. The pellet was resuspended in 10 mM Tris-HCl (pH 7.5), 10 mM NaCl, and 1 mM EDTA (buffer I), and the cells were lysed by passage through a French Press. The material was then cleared by centrifugation, and the decanted supernatant was designated as fraction I. The protein concentration was determined by the method of Bradford (*25*) using BSA as a standard.

Fraction I GFPP was dialyzed into imidazole-binding buffer, and the N-terminal hexahistidine affinity tag was used to purify GFPP according to the instructions supplied in the His-tag purification kit (Novagen, Inc.). This material that eluted from the His-tag affinity column was pooled and extensively dialyzed against buffer I. The dialyzed material was designated as fraction II.

If required, fraction II was applied to a Sephadex G-75 column (110 cm × 7.6 cc^2). Peak fractions were pooled after fraction aliquots were visualized by SDS−PAGE. The G75 pool was designated as fraction III and represented homogeneous GFPP protein. Fraction III GFPP protein was concentrated as required by pressure filtration through a semipermeable membrane (Amicon YM-3) and dialyzed into various buffers.

Synthesis of Radiolabeled Substrates. [γ-^{32}P]ATP was purchased from ICN Biomedicals, Inc. The first step toward the synthesis of GDP-fucose analogues was the preparation of [^{32}P]fucose-1-phosphate. This was typically achieved by combining the following in a 500 μL reaction: 20 mM fucose, 20 mM [γ-^{32}P]ATP, 10 mM Tris-HCl at pH 7.0, 5 mM EDTA, 50 mM NaCl, 15.0 mM $MgCl_2$, and 2.5 units of fucose kinase (E. C. 2.7.1.52). A laboratory recombinant source of human fucose kinase was employed. The reaction was incubated at 37 °C for 4 h at which time we added 100 μL of an acidic suspension of Norit A. The mixture was incubated on ice for 5 min and centrifuged at 14000*g* for 15 min. The supernatant was collected and recentrifuged as above. The resulting supernatant was neutralized by the addition of NaOH to a final pH of 7.0. Purity was assayed via ^{31}P NMR, ($CDCl_3$) δ: −1.23. This material was used to form NDP-β-L-fucose with various GTP analogues.

[γ-^{32}P]GTP was purchased from ICN Biomedicals, Inc. The material was treated with an acidic suspension of Norit A on ice for 30 min. The mixture was then centrifuged at 14000*g* for 10 min. The supernatant was removed, and the pellet was resuspended in cold water. The mixture was recentrifuged and rewashed with cold water two more times. The [γ-^{32}P]GTP was eluted from the Norit A by the addition of concentrated ammonium hydroxide in 50% ethanol. After a 10 min incubation on ice, the mixture was centrifuged as above and the supernatant was decanted. The pH was adjusted to 7.0 by the addition of HCl. This material was used to form NDP-β-L-fucose with various hexose-1-phosphate analogues.

Synthesis of Fleximer and Tricyclic Nucleoside Triphosphates. The guanosine fleximer nucleoside and the guanosine and inosine tricyclic nucleosides were synthesized as previously described (*26*, *27*). The three nucleosides were converted into their respective triphosphate forms via the combination of enzymatic and chemical methodologies. Each nucleoside was phosphorylated by *Escherichia coli* guanosine-inosine kinase (GSK, E. C. 2.7.1.73). A typical reaction contained 10 mM nucleoside, 40 mM $MgCl_2$, 20 mM $MnCl_2$, 40 mM Tris-HCl (pH 7.2), 50 mM urea, and 20 mM ATP in a final volume of 500 μL. GSK produced from a laboratory clone was added to a final protein concentration of 0.1 mg mL^{-1}. The reaction mixture was incubated at 30 °C for 48 h with occasional agitation. ADP was separated from the NMP species via anion-exchange chromatography using a Whatman Partisil 10 SAX column. A linear gradient from 20 mM NaH_2PO_4 (pH 4.5) to 800 mM NaH_2PO_4 (pH 4.5) was employed. Fractions containing the MNP were pooled and desalted via size-exclusion chromatography on a 5 cm × 0.78 cc^2 Bio-Gel P-2 column run in water. NMP-containing fractions were pooled and brought to dryness overnight. Typically these steps were done in batches to ensure that enough material was available for conversion to the triphosphate. The dried material was

dissolved in a minimum volume of anhydrous DMF and was returned to dryness twice. Alternatively, the monophosphate reaction product could be separated from the ADP by reverse-phase chromatography through a Waters Nova-Pack column using 50 mM triethylamine phosphate (pH 6.5) as the mobile phase. The formation of the triphosphate species employed the technique of Moore et al. (*28*). The overall yield, as determined by UV absorbance, was approximately 35%.

Each sample preparation was verified by ^{31}P NMR. For this analysis, a small amount of solid material was resuspended in D_2O. NMR analysis was carried out using a Bruker 500 MHz NMR. NTP molecules feature three resonances (with respect to a H_3PO_4 external standard) at approximately −6, −11, and −22 ppm. These correspond to the γ, α, and β phosphorus atoms, respectively (*29*). Specific resonances: guanosine fleximer, −9.31, −10.05, and −21.92; inosine fleximer, −9.12, −10.13, and −22.22; and tricyclic guanosine, −8.87, −10.27, and −21.78.

Enzymatic Assays. The first procedure measures the hydrolysis of [γ-^{32}P]GTP to Norit nonadsorbable $^{32}PP_i$ and was used in the reactions involving modified hexose moieties (meaning reactions involving unmodified guanine as the nucleotide base). The reaction conditions include, in 100 μL, 50 μM [γ-^{32}P]GTP at 100 nCi, 20 mM Tris-HCl at pH 7.0, 10.0 mM $MgCl_2$, 1 mM fucose-1-P (or other hexose-1P), and various amounts of enzyme. Back reactions were prevented by the inclusion of 0.01 units of yeast inorganic pyrophosphatase. After 20 min at 37 °C, the reaction was terminated by addition of an acidic suspension of Norit A. The reaction was centrifuged at 8000*g*, and an aliquot of the supernatant was assayed via scintillation counting. For reactions employing different (nonradioactive) NTPs, a second procedure was employed. The reaction conditions include, in 100 μL, 100 μM [^{32}P]fucose-1-phosphate at 300 nCi, 20 mM Tris-HCl at pH 7.0, 15.0 mM $MgCl_2$, 1 mM NTP, and various amounts of enzyme. Back reactions were prevented by the inclusion of 0.01 units of yeast inorganic pyrophosphatase. After 20 min at 37 °C, the reaction was terminated by the addition of an acidic suspension of Norit A and centrifuged as above. The supernatant was discarded, and the pellet was resuspended in 100 μL of cold water. An aliquot of this mixture was counted on a scintillation counter. Kinetic parameters were calculated according to Segel (*30*).

The reaction procedure follows the formation of the nucleotide−sugar by measuring Norit adsorbable radioactivity in the presence of unlabeled NTPs and ^{32}P-labeled fucose-l-P. In this scenario, the newly synthesized nucleotide−sugar will contain the radiolabel and pellet with the Norit. The unreacted radioactive fucose-l-P remains in the supernatant and is easily separated from the radioactivity in the Norit pellet by a series of washing/decanting steps. The selective ability of acidified Norit to adsorb any nucleobase-containing compound means that the same assay can be used with γ-^{32}P-GTP and unlabeled hexose. In this case, the radiolabel is released in the form of pyrophosphate and is counted in the supernatant. Unreacted γ-^{32}P-GTP partitions in the Norit pellet.

Isothermal Titration Calorimetry (ITC). ITC was performed with a VP-ITC instrument from MicroCal, Inc. Titrations were carried out by injecting 5 μL of an NDP−sugar solution (at concentration ranges from 0.25 to 1.0 mM) into the 1.4 mL stirred reaction cell. GFPP ranged in concentration from 50 to 80 μM in the cell. Both the nucleotide−sugar and the enzyme were in 20 mM sodium cacodylate (pH 5.5−7.0) and 40 mM NaCl or 20 mM Tris-HCl (pH 7.0−7.5) and 40 mM NaCl. Titrations were conducted between 20 and 40 °C. Typical experimental conditions for the titrations were a 10 s injection period followed by a 240 s delay between injections for a total of 40 injections. Blank titrations of inhibitor into buffer were performed to correct for heats of dilution and mixing. The independent set of multiple binding sites is the most common model for binding experiment evaluations. The analytical solution for the total heat used in this study was as described by Freire et al. (*31*). Data were fit to this model using Origin version 7 (MicroCal, Inc.).

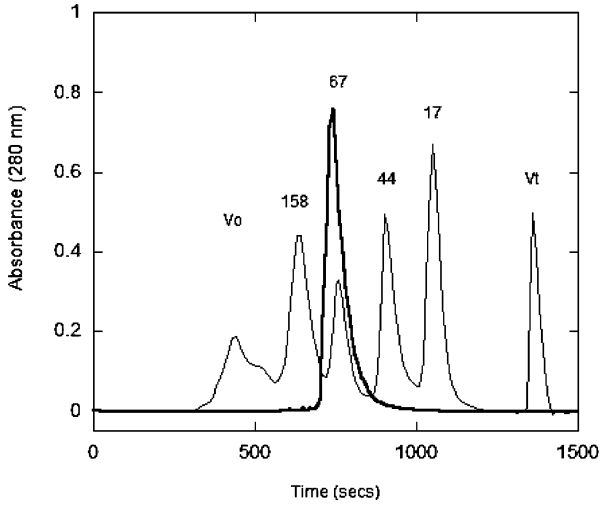

FIGURE 1: Size-exclusion chromatography through a 30 × 0.78 cm Bio-Silect 250 column. Human GFPP elution profile superimposed on molecular weight standards. The size of the standards is indicated: thyroglobin (V_o, void volume); γ globulin, 158 kDa; BSA, 67 kDa; ovalbumin, 44 kDa; myoglobin, 17 kDa; ATP (volume total, V_t).

RESULTS

Cloning and Enzyme Purification. A full-length clone encoding human GFPP was successfully isolated from a prepared liver cDNA library and cloned into pET15b. The insert was fully sequenced and found to be identical to the published sequence (*14*). The purification of GFPP from *E. coli* results in approximately 5 mg of protein per liter of induced culture. The purification regime outlined in the Experimental Procedures takes approximately 2 days to complete. GFPP is overproduced approximately 27-fold in *E. coli*. In the course of the purification, GFPP-containing fractions could be pooled solely based on SDS−PAGE gel visualization. The enzyme is not stable when the frozen cell paste is disrupted via French press in the presence of imidazole-binding buffer (data not shown). To alleviate this issue, crude protein extract was prepared in buffer I followed by dialysis into binding buffer in preparation for the nickel-affinity purification step. The material that elutes from the nickel column contains several contaminating proteins. These were efficiently removed via size-exclusion chromatography.

The chromatographic behavior of GFPP on a Bio-Silect 250 gel-exclusion column (Bio-Rad, Inc.) is shown in Figure 1. The chromatogram was consistent with a monomeric

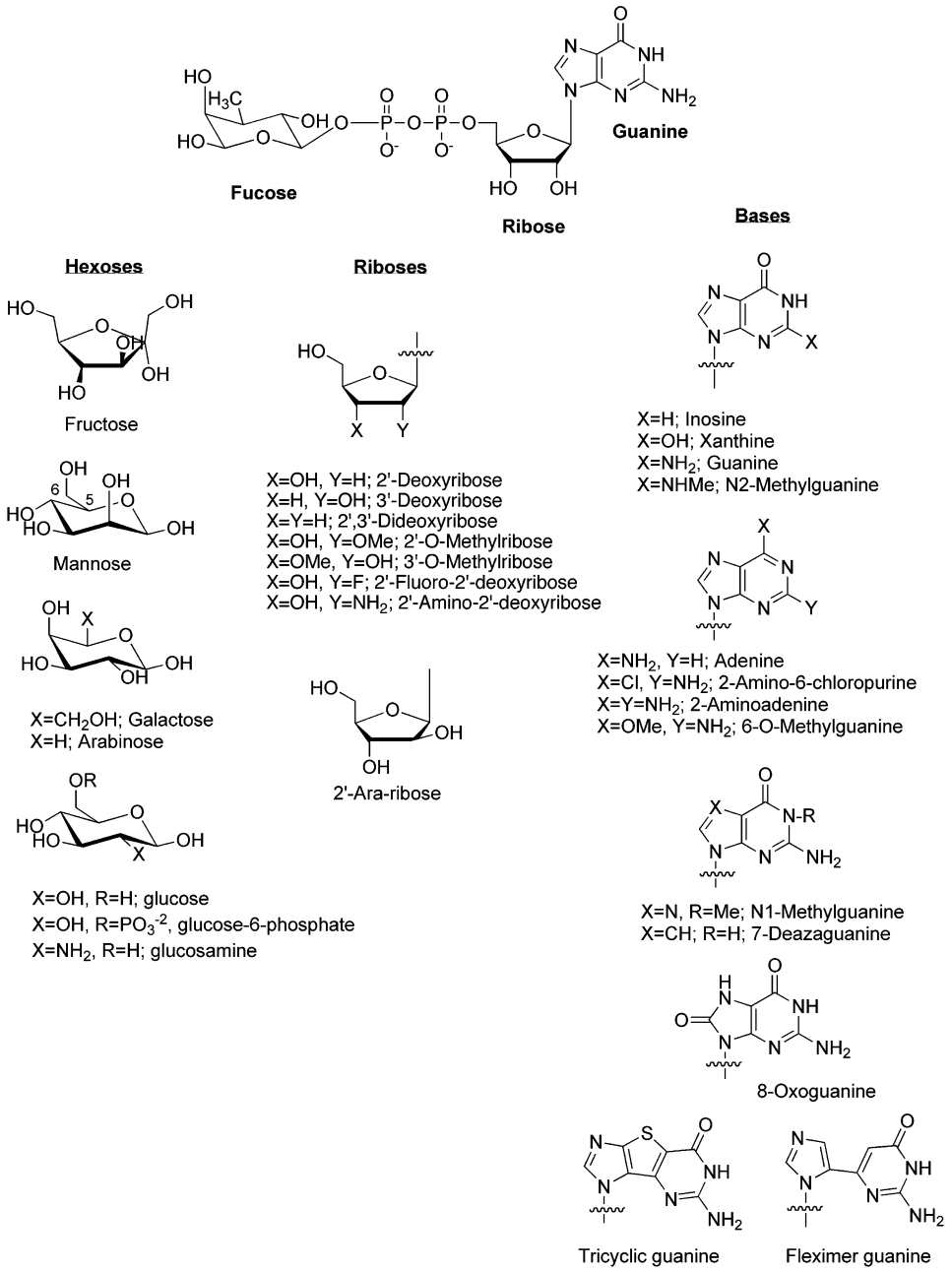

FIGURE 2: Structure of the substrate analogues used in this study.

protein, as was expected. The previously identified porcine GFPP is a monomer (*14*). Analytical gel-filtration experiments (Figure 1) indicate that the GFPP protein elutes from the column slightly before a bovine serum albumin standard (67 kDa). The elution profile is consistent with the protein being a monomer with a molecular weight of approximately 66.6 kDa. The calculated Stokes radius is 34 Å. The elution profile suggests that the protein is primarily symmetric in nature because the frictional coefficient is 1.2. This does however indicate a slight degree of oblate spheroid character. The elution profile of GFPP was the same whether the enzyme was bound to substrates.

Enzymology and Substrate Recognition. Figure 2 illustrates the base-, hexose-, and ribose-modified nucleotide−sugars that were investigated as part of this study. Table 1 shows the K_m and k_{cat} values for a series of guanine-like bases. In this portion of the present work, a NTP nucleobase analogue was used, in conjunction with fucose-1-phosphate to dissect base discrimination. The K_m for a guanine base (as in GTP) is 50 μM with a turnover of 2.5 s^{-1}. Clearly, the best canonical base part of a substrate is guanine with a catalytic efficiency of 49.8 μM^{-1} s^{-1}. The second best base part of a substrate is 8-oxoguanine with a catalytic efficiency of 40.8 μM^{-1} s^{-1}. Most of the base parts of the NTP molecule are in fact poor substrates. This is reflected both in binding (k_m) and catalysis (k_{cat}). Even though the base-substituted NDP-β-L-fucose molecules are not good substrates, a pattern of base recognition emerges from the data presented in Table 1. This discrimination is best illustrated by comparing the ratio of catalytic efficiency (the value *D* in Table 1). GFPP discriminates base substrate from nonsubstrate primarily by sensing a potential hydrogen-bonding face that is made by the carbonyl oxygen at C-6, the N-1 ring nitrogen, and the exocyclic amino group. Of the three base determinants, the primary determinant seems to be the exocyclic amino group. GFPP discriminates between guanine (as in GTP) and *N*2-

Table 1: Enzymology of Nucleoside Triphosphate Substituted NDP-β-L-fucose

nucleoside analogue of the NTP	K_m (μM)	k_{cat} (s^{-1})	k_{cat}/K_m ($\mu M^{-1}\ s^{-1} \times 10^3$)	D[a]
guanine	50.2 (1.8)[b]	2.5 (0.1)	49.8	1.0
7-deazaguanine	75.4 (1.2)	1.5 (0.1)	19.9	2.5
*N*1-methylguanine	423 (3.6)	0.02 (0.001)	0.05	996
*O*6-methylguanine	121.1 (3.9)	0.09 (0.002)	0.74	67.3
8-oxoguanine	63.6 (1.4)	2.6 (0.1)	40.8	1.2
*N*2-methylguanine	1,263 (7.8)	0.009 (0.001)	0.001	49 800
fleximer guanine	39.8 (0.7)	3.5 (0.1)	87.9	0.57
tricyclic guanine	232 (2.4)	0.29 (0.03)	1.3	38.3
inosine	61.6 (1.9)	1.2 (0.2)	19.5	2.6
xanthine	823.1 (3.1)	0.03 (0.005)	0.04	1245
adenine	516.3 (6.1)	0.009 (0.001)	0.02	2490
2-aminoadenine	210.0 (6.1)	0.32 (0.02)	1.5	33.2
2-amino-6-chloropurine	163.9 (1.7)	0.27 (0.04)	1.6	31.1

[a] D is the discrimination factor and is defined as $(k_{cat}/K_m)^{sub}/(k_{cat}/K_m)^{ana}$, where "sub" refers to the natural GFPP substrate, GDP-L-fucose and "ana" refers to an analogue nucleotide−sugar. [b] The value shown is the mean of three replicate experiments. The number in parentheses is the standard deviation.

methylguanine (as in N2-MeGTP) by a factor of 49 800 during the formation of NDP-β-L-fucose. Similarly, the enzyme is less capable of using xanthine (XTP, $D = 1{,}245$) as a substrate, although inosine (as in ITP) is utilized to an appreciable extent ($D = 2.6$).

Coupled with the exocyclic amino group is the role that is played by the carbonyl at C-6 of the purine ring. When adenine is the base, substituted NTP (as in ATP) is an extremely poor substrate, with barely discernible ability to act as a substrate during synthesis ($k_{cat} = 0.009\ s^{-1}$).

GFPP is less efficient in using 2-aminoadenosine triphosphate as a substrate ($D = 33.2$). No measurable enzymatic activity could be detected when the substituent at the 6 position was altered to a halogen, as in 6-chloroadenosine triphosphate (data not shown), but 2-amino-6-chloropurine ($k_m = 163.9\ \mu M$, $k_{cat} = 0.27\ s^{-1}$, and $D = 31.1$) was used as efficiently by GFPP as 2-aminoadenosine triphosphate ($k_m = 210\ \mu M$, $k_{cat} = 0.32\ s^{-1}$, and $D = 33.2$).

Hydrogen bonding at the N-1 nitrogen is the last component in this recognition face. It in part helps to explain GFPP discrimination between guanine- and adenine-based nucleotides. If all three of these groups are removed, as in benzimidazole triphosphate, no enzymatic activity or binding is seen (data not shown). GFPP does not strongly recognize constituents on the imidazole portion of the purine base as a method of distinguishing the substrate from the nonsubstrate. This is exemplified in 7-deazaguanosine, where removal of the N-7 nitrogen only slightly affects enzymatic efficiency ($k_m = 75.4\ \mu M$, $k_{cat} = 1.5\ s^{-1}$, and $D = 2.5$). Adding a methyl group at N-1 does result in a large decrease in the ability of GFPP to form N1-methylGDP-β-L-fucose ($k_m = 423\ \mu M$, $k_{cat} = 0.02\ s^{-1}$, and $D = 996$), but this may be primarily due to unfavorable steric interactions in the active site. This seems a plausible explanation especially when one considers the activity exhibited by 7-deazaguanosine triphosphate, as well as the observation that 8-oxoguanosine triphosphate is nearly as good of a substrate as GTP ($D = 1.2$). The enzyme can effectively utilize a wide variety of guanine analogues. The fleximer guanine base (Figure 2 and Table 1) is actually a better substrate for the enzyme than is a canonical guanine ($k_m = 39.8\ \mu M$, $k_{cat} = 3.5\ s^{-1}$, and $D = 20.57$). Similarly, the tricyclic guanine base (Figure 2 and Table 1) can be utilized ($k_m = 232\ \mu M$, $k_{cat} = 0.29\ s^{-1}$, and $D = 38.3$).

Table 2: Enzymology of Hexose- and Ribose-Substituted GDP-Sugar

compound	K_m (μM)	k_{cat} (s^{-1})	k_{cat}/K_m ($\mu M^{-1}\ s^{-1} \times 10^3$)	D[a]
hexose-1-P substitutions				
fucose	67.0 (1.1)[b]	3.6 (0.1)	53.7	1.0
glucose	346.4 (0.7)	0.32 (0.03)	0.92	58
glucose-6-phosphate	621.3 (0.4)	0.18 (0.02)	0.29	185
mannose	542.5 (0.4)	0.20 (0.02)	0.37	145
glucosamine	828.8 (0.3)	0.21 (0.02)	0.25	215
galactose	676.7 (0.4)	0.23 (0.02)	0.34	158
fructose	823.2 (0.2)	0.03 (0.01)	0.04	1343
arabinose	85.4 (1.1)	0.4 (0.03)	4.7	11
ribose substitutions				
ribose	50.2 (1.8)	2.5 (0.1)	49.8	1.0
2′-deoxyribose	83.7 (1.5)	0.3 (0.04)	3.6	13.8
3′-deoxyribose	75.6 (1.6)	2.1 (0.1)	27.8	1.8
2′,3′-dideoxyribose	118.0 (0.8)	0.04 (0.001)	0.33	151
2′-*O*-methylribose	123.2 (0.7)	0.2 (0.02)	1.6	31.3
2′-ara-ribose	66.6 (0.3)	0.26 (0.03)	3.9	12.8
2′-fluoro-2′-deoxyribose	42.6 (0.5)	0.009 (0.001)	0.21	237
2′-amino-2′-deoxyribose	68.9 (0.7)	0.05 (0.003)	0.73	68.2
3′-*O*-methylribose	55.3 (0.3)	1.6 (0.2)	28.9	1.7

[a] D is defined in the footnote of Table 1. [b] The value shown is the mean of three replicate experiments. The number in parentheses is the standard deviation.

GFPP displays very specific hexose discrimination. In this portion of the study, unmodified GTP was reacted with various hexose-1-phosphates to dissect portions of the hexose that are important for binding or catalysis. The K_m for fucose is 67 μM with a k_{cat} of 3.1 s^{-1}. None of the hexoses tested in Table 2 were appreciably utilized by GFPP, although some enzymatic activity is measurable for all of them. Enzymatic efficiency was decreased 11−1343-fold, with turnover being reduced for most of the hexoses approximately 13-fold. The primary site for GFPP discrimination of potential hexose substrates is the methyl group at position C-6. If this is missing, the hexoses cannot be efficiently used as substrates. Substituting the methyl with an ethyl group, as in galactose, has a similar effect to leaving it off ($k_m = 676.7\ \mu M$, $k_{cat} = 0.23\ s^{-1}$, and $D = 158$). Similar activity is seen when mannose is used as the hexose-1-phosphate ($k_m = 542.5\ \mu M$, $k_{cat} = 0.2\ s^{-1}$, and $D = 145$). The stereochemistry of the hydroxyl group at C-5 is the second site of substrate discrimination. Of all of the hexoses employed in this study, only arabinose displays the same stereochemistry as fucose at this position. Arabinose can serve as a substrate ($k_m = 85.4\ \mu M$, $k_{cat} = 0.4\ s^{-1}$, and $D = 11$), even though it is missing the C-6 methyl group, primarily because of the C-5 hydroxyl. Removal of this hydroxyl is extremely detrimental to the ability of GFPP to use a hexose (e.g., fructose ($k_m = 823.2\ \mu M$, $k_{cat} = 0.03\ s^{-1}$, and $D = 1343$), as a substrate.

Finally, GFPP is capable of utilizing a wider variety of ribose moieties. In this portion of the study, various ribose-substituted GTP moieties were reacted with fucose-1-P to look at the effect of ribose substitutions on binding or catalysis. The results in Table 2 show that the only ribose substituent that plays a role in substrate recognition is the 2′-hydroxyl, although the enzyme can catalyze the formation of GDP-β-L-fucose from 2′-deoxyribose GTP ($D = 13.8$). Substitutions at the 3′ position had little effect on discrimina-

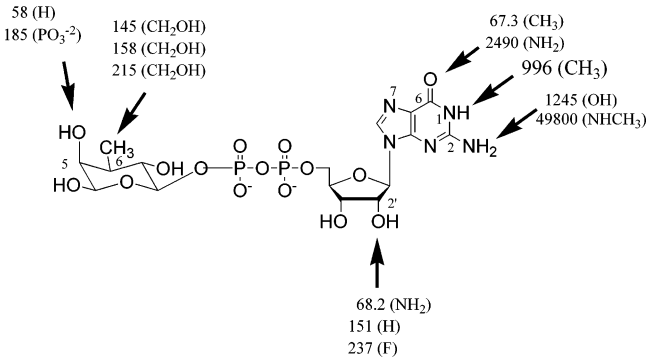

FIGURE 3: Diagram showing the molecular recognition constituents that help GFPP discriminate the substrate from the nonsubstrate during the synthesis of nucleotide−sugars. Shown is the structure of GDP-β-L-fucose. Numbers at each arrowed position refer to the discrimination factor for specific substitutions (in parentheses) at that position. Refer to Tables 1 and 2 for details.

tion by the enzyme (3′-deoxyribose, $D = 1.8$; 3′-*O*-methylribose, $D = 1.7$). One 2′- or 3′-hydroxyl is preferred, but not required, because even 2′,3′-dideoxyribose ($D = 151$) can be utilized to some extent. The conformation of the 2′-hydroxyl was as critical to enzyme discrimination (2′-arabinose, $D = 12.8$) as not having a hydroxyl at that position. Finally, changing the 2′-hydroxyl group to either a fluorine ($D = 237$) or an amino group ($D = 68.2$) was deleterious to the ability of GFPP to utilize the substrate.

To summarize, GFPP discriminates between the substrate and the nonsubstrate by recognizing the C-6 fucose methyl group, the substituent (and stereochemistry) at the C5 and the C3 positions of the hexose, as well as a specific hydrogen-bonding surface on the heterobase, made up of the C-6 carbonyl, the N-1 nitrogen, and the C-2 exocyclic amine group. Finally, GFPP senses the substituent on the 2′-ribose position. These features are shown in Figure 3.

Calorimetric Binding Analysis. ITC has proven to be an invaluable tool for the study of enzyme active-site architectures. This is especially true when the three-dimensional structure of the enzyme is unknown or when there are no sequence homologues of known structure to study. Figure 4 shows a typical binding isotherm, in this case for the titration of GFPP with GDP-β-L-fucose. Binding of nucleotide−sugar analogues to GFPP is an exothermic process, but there is a wide variation in both the enthalpic and entropic contributions to that binding. The thermodynamic parameters are summarized in Table 3. For the majority of nucleotide−sugar analogues, binding to GFPP is entropically unfavorable. This may indicate that there is an associated change in the heat capacity upon binding. Measurements of ΔH and ΔG as a function of the temperature (representative data shown in Figure 5) indicate that ΔH is temperature-dependent. There is a linear relationship between the binding enthalpy and the temperature over the temperature range tested. These data were used to calculate the binding-induced change in the heat capacity (Table 3). Values of ΔC_p range from −585 cal mol^{-1} K^{-1} for fleximerGDP-fucose to −85 cal mol^{-1} K^{-1} for GDP-arabinose. For the analogues that are entropically unfavorable, the ΔG of binding is nearly independent of the temperature, whereas when nucleotide−sugar binding is entropically favorable, the ΔG of binding shows some temperature dependence.

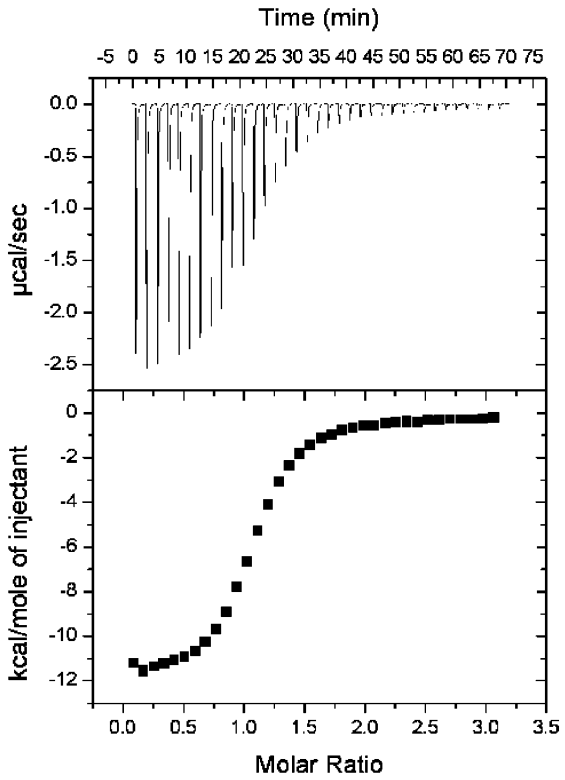

FIGURE 4: Typical ITC binding analysis between GFPP and NDP−sugars. In this case, data are shown for GDP-β-L-fucose binding to the enzyme. The nucleotide−sugar was dissolved in 20 mM cacodylate (pH 7.0) and 20 mM NaCl at a final concentration of 1 mM. GFPP was dialyzed in the same buffer and was used in the calorimeter cell at a concentration of 20 μM. The temperature was maintained at 20 °C, and 40 injections of 5 μL each were employed with a 240 s re-equilibrium time between injections. (Top panel) Each peak shows the heat produced by the injection and subsequent binding reaction. (Bottom panel) Binding isotherm produced by integrating each injection peak with respect to time. Shown is the enthalpy per mole of GDP-β-L-fucose injected versus the GDP-β-L-fucose/GFPP molar ratio.

Not surprisingly "guanosine-like" bases bind with higher affinity than do other base analogues. The base recognition rules that were elucidated with the enzymological study are mirrored with the ITC-binding data. The fleximer guanine base binds to the enzyme with higher affinity ($K_a = 7.3 \times 10^6$ M^{-1}) than does canonical guanine ($K_a = 4.6 \times 10^6$ M^{-1}). Among the bases tested in this study, adenine binds with the lowest affinity ($K_a = 2.0 \times 10^4$ M^{-1}). Bases with very low affinities (adenine and xanthine) bind to GFPP with a favorable entropic term ($\Delta S = 8.7$ and 6.7 cal mol^{-1} K^{-1}, respectively). A similar phenomenon is seen with the low affinity binders arabinose ($K_a = 1.0 \times 10^4$ M^{-1}; $\Delta S = 9.4$ cal mol^{-1} K^{-1}) and 2′-fluoro-2′-deoxyribose ($K_a = 2.0 \times 10^4$ M^{-1}; $\Delta S = 1.7$ cal mol^{-1} K^{-1}). There is generally good correlation between K_d and K_m for the data presented.

DISCUSSION

L-Fucose is an important monosaccharide in bacteria, plants, and mammals (for a review, see ref *1*). It is a major constituent of glycoproteins and glycolipids and has been associated with several human disease states (e.g., ref *8*), tumor metastasis (*32*), fertilization (*33*), and apoptosis (*34*). The inclusion of L-fucose into glycolipid or glycoprotein structures requires the use of a nucleotide−sugar intermediate, namely, GDP-β-L-fucose. In mammals, two pathways operate to produce GDP-β-L-fucose. A *de novo* constitutive

Table 3: Binding Thermodynamics of Nucleotide−Sugar Substrate Analogues and Inhibitors

compound	n	K_a ($M^{-1} \times 10^6$)	ΔH (kcal mol^{-1})	ΔS (cal mol^{-1} K^{-1})	ΔG (kcal mol^{-1})	ΔC_p[a] (cal mol^{-1} K^{-1})
NDP-β-L-fucose						
guanine	0.98 (0.03)[b]	4.6 (0.8)	−14.5 (1.2)	−19.4 (1.8)	−8.7 (0.6)	−536 (112)
7-deazaguanine	1.03 (0.04)	4.4 (0.9)	−12.8 (1.1)	−17.4 (1.5)	−7.6 (0.4)	−419 (101)
8-oxoguanine	1.01 (0.02)	4.2 (0.9)	−13.9 (0.8)	−20.6 (1.7)	−7.7 (0.4)	−457 (111)
fleximer guanine	0.96 (0.04)	7.3 (0.7)	−17.2 (0.7)	−16.3 (0.9)	−12.3 (0.5)	−585 (121)
tricyclic guanine	1.03 (0.03)	0.5 (0.04)	−11.2 (0.6)	−21.1 (1.6)	−4.9 (0.2)	−366 (92)
adenine	1.08 (0.05)	0.02 (0.01)	−5.8 (0.9)	8.7 (1.1)	−8.4 (0.3)	−242 (63)
xanthine	0.95 (0.08)	0.21 (0.09)	−7.2 (0.7)	6.7 (0.8)	−9.2 (0.4)	−229 (58)
GDP-sugar						
glucose	1.07 (0.05)	0.31 (0.08)	−14.2 (1.1)	−23.6 (1.2)	−7.1 (0.4)	−372 (92)
arabinose	0.98 (0.04)	0.01 (0.003)	−3.5 (0.6)	9.4 (0.9)	−6.3 (0.2)	−85.3 (21)
fructose	1.10 (0.05)	0.88 (0.07)	−10.4 (1.6)	−24.1 (1.4)	−3.2 (0.1)	−338 (91)
GDP-ribose-β-L-fucose						
3′-deoxyribose	1.07 (0.02)	2.3 (0.6)	−13.6 (0.7)	−16.3 (0.9)	−8.7 (0.5)	−440 (123)
2′-fluoro-2′-deoxyribose	0.96 (0.03)	0.02 (0.001)	−4.9 (1.5)	1.7 (0.04)	−5.4 (0.3)	−131 (45)

[a] Calculated from $\Delta C_p = (\Delta H_{T_2} - \Delta H_{T_1})/(T_2 - T_1) = (\Delta S_{T_2} - \Delta S_{T_1})/(\ln(T_2/T_1))$. [b] The value shown is the mean of three replicate experiments. The number in parentheses is the standard deviation.

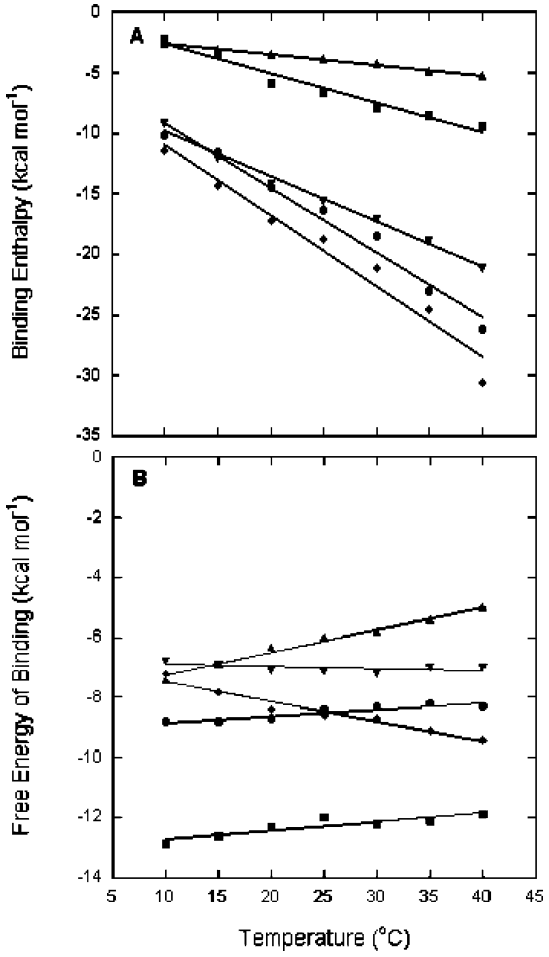

FIGURE 5: Temperature dependence of the enthalpy of binding (A) and the free energy of binding (B) for selected nucleotide−sugars binding to GFPP. The parameters have been corrected for buffer ionization. The data points were measured by ITC as described in the Experimental Procedures. The heat capacity change that is associated with nucleotide binding was calculated as the slope of a linear fit of ΔH versus temperature. For both panels, the closed symbols are GDP-β-L-fucose, ●; ADP-fucose, ■; fleximerGDP-fucose, ◆; GDP-arabinose, ▲; GDP-glucose, ▼.

pathway (*34*) converts GDP-α-D-mannose to GDP-β-L-fucose by the action of GDP-D-mannose-4,6-dehydratase (E. C. 4.2.1.47) and GDP-4-keto-6-deoxy-D-mannose-3,5-epimerase-4-reductase (E. C. 1.1.1.271). A second two-step salvage pathway produces GDP-β-L-fucose from free fucose and GTP. The first step of the overall reaction is catalyzed by an ubiquitous fucose kinase (E. C. 2.7.1.52; *38*) that forms L-fucose-1-P from fucose and ATP. The second step in the overall reaction is catalyzed by GFPP utilizing the L-fucose-1-P and GTP (*14*).

Given the importance of fucose metabolism in cellular physiology (both eukaryotic and bacterial) and in host parasite interactions, it is important to fully understand the enzymes involved in the utilization of the sugar. Fucose kinase has been studied in detail, but other than cloning and initial characterization studies, little work has been done on GFPP. This is in stark contrast to other nucleotide−sugar pyrophosphorylases (e.g., refs *35*−*37*). Even though the salvage pathway may only account for 10% of the total cellular GDP-β-L-fucose pool (*38*), several studies (*14*, *39*) indicate that GFPP and fucose kinase are expressed at high levels in many tissues. Therefore, they clearly play a more significant role in the overall synthesis of GDP-β-L-fucose. GFPP may also be a new target for anti-inflammatory and antimetastatic drugs. This work clearly demonstrates that although the GFPP active site is plastic, the enzyme is only significantly active when naturally occurring substrates include guanine, ribose, and fucose. This ensures that the salvage pathway is very specific for GDP-β-L-fucose, and it does not deleteriously impact other nucleotide−sugar metabolism.

Using a broad range of nonnatural substrate analogues, GFPP can efficiently form nucleotide−sugars from a series of guanine-like bases. The modified enzyme assay simplifies experiments and allows for the testing of a broader range of potential substrate molecules. Using this assay, it was possible to measure K_m values to the millimolar range (from the submicromolar range) and turnover as low as 0.001 s^{-1}. The discrimination factor, D, the ratio of the natural substrate catalytic efficiency with that of the analogue, has proven a useful metric when comparing the impact of base modifications on binding and enzymatic turnover. Values of D greater than unity indicate that the analogue is a less efficient substrate for the enzyme than the natural substrate.

The polarity of the hydrogen-bonding surface about the base is the critical determinant in base recognition. The polarity of GTP is obviously preferred. The pattern of

hydrogen bonding is switched in ATP relative to GTP by the inversion of the carbonyl and exocyclic amino group positioning. This indicates the importance of these specific hydrogen-bonding partners in determining base substrate preferences. The C-6 carbonyl is a major base substrate determinant, because no enzymatic activity could be detected when 2-amino-adenosine triphosphate was used as a substrate, even though the exocyclic amino group was properly in position 2. When the carbonyl oxygen is blocked, as in *O*-6-methyl guanosine triphosphate, some enzymatic activity could be detected in the assay, but it is much less efficient. This again shows the interplay between substituents at the C-2 and C-6 ring positions. Similar guanine base hydrogen-bonding surfaces have been implicated in substrate recognition with other GTP-binding proteins (*40*). Consistent with the base discrimination hypothesis is the observation that 2-aminoadenosine triphosphate can be utilized as a substrate. In this case, the C-2 exocyclic amino group inherent in guanosine is present, but the C-6 carbonyl of guanine has been replaced by the C-6 exocyclic amine normally present in adenine.

The active site of GFPP displays a surprising degree of plasticity. The enzyme is very active when the guanosine fleximer triphosphate is used as a substrate. In fact, fleximer GTP is a slightly better substrate than is GTP ($D = 0.57$). This analogue was originally designed (*26*) to allow a greater degree of flexibility during binding by separating the two purine base constituents by a single carbon−carbon bond, while retaining the hydrogen-bonding components necessary for recognition. It was hoped that this modified base would show adaptability for diverse enzyme active sites by allowing free rotation of the two ring components. Whether fleximer GTP adopts a different binding geometry than GTP in the GFPP active site will ultimately be solved crystallographically. However, at a minimum, the GFPP active site that shows a high degree of discrimination for guanosine-like bases can accommodate a guanosine base analogue that is 1.5 Å longer than the canonical base and utilize it better than GTP. This increase is manifested both in binding (K_m) and enzymatic turnover (k_{cat}). More dramatically is the ability of GFPP to utilize tricyclic guanosine triphosphate as a substrate. This molecule (see Figure 2) again separates the purine ring components by 1.5 Å but, unlike the fleximer guanosine, locks the ring into a rigid conformation. Tricyclic GTP binds less readily in the GFPP active site than GTP and is harder to utilize as a substrate once bound, but GFPP can employ this molecule as a substrate with a fair degree of efficiency ($D = 38.3$). Again the driving force behind base recognition seems to be a "guanosine-like" hydrogen-bonding surface where polarity of those interactions is maintained. If all three are present, the molecule can be effectively utilized (even if the purine ring is split). If two are present, then GFPP can use these molecules with relatively similar efficiency. If the polarity of these groups is reversed or they are all abolished, then GFPP cannot utilize these base analogues as substrates. It may also be surprising that the enzyme is competent to handle a large array of guanine-like bases, yet the analogues used in the study are very closely related to guanine. Pyrimidines or analogues more structurally removed from guanine are not substrates (data not shown). This model system therefore allows for a more subtle evaluation of substrate constituents.

For all of the analogues tested in this study, there was a positive but nonlinear correlation between K_m and k_{cat}. That is, the harder it was for the substrate to bind to the enzyme (as seen by alterations in the Michaelis constant), the slower the catalytic step (as seen by changes to the value of the catalytic constant). The fact that the K_m-k_{cat} relationship is not linear indicates that there is a more complicated interrelationship between the kinetics and thermodynamics of substrate binding (*41*). This also indicates that some bound substrate leaves the active site via dissociation rather than through formation of a nucleotide−sugar. The enzyme is active in the presence of substoichiometric amounts of magnesium ion. This means that ITC analysis is not possible in the presence of metal because thermodynamic parameters associated with substrate binding are confounded by substrate hydrolysis during the binding time course (data not shown). It is known that the exact magnitude of thermodynamic parameters can vary in the presence or absence of metal ion, but the general thermodynamic trends remain the same. A detailed thermodynamic analysis of metal−enzyme−substrate binding is underway using a variety of metals that promote substrate binding but do not support catalysis (manuscript in preparation).

There is strong enthalpy−entropy compensation for most analogues, especially those that bind with unfavorable entropy. The large ΔC_p results from the weak temperature dependence of ΔG and the strong enthalpy−entropy compensation. This indicates that binding is accompanied by alterations in the solvent-accessible surface area of GFPP. The result indicates that the interaction between GFPP and most nucleotide−sugars is enthalpically driven; that is, ΔH is negative. The reaction is not favored entropically as evidenced by the negative value of ΔS. However, the enthalpic term is larger in magnitude than the term, $T\Delta S$; hence, the overall free energy of binding is negative.

Surprisingly, a few of the substrate analogues bind to GFPP with a favorable entropic term. Subsequent analysis indicates that, in these analogues, ΔH is only partially compensated for by the $T\Delta S$ and that ΔG is more temperature-dependent (ΔC_p is not as significant too). There is a good correlation between the ability of GFPP to utilize a particular set of substrates and the ΔC_p. The less a substrate (meaning the NTP or the hexose) can be used efficiently as a substrate, the lower the value of the heat capacity change upon binding. Oddly, there is also a direct correlation between the ability of GFPP to form a particular nucleotide−sugar and the binding entropy. The reason behind this observation is unclear but indicates that the thermodynamics of binding may be more complicated. The overall negative binding enthalpy indicates that electrostatic interactions may predominate the binding reaction, perhaps including desolvation of GFPP side chains (*42*). Positive (favorable) ΔS values usually arise from the release of ordered water molecules into the bulk solvent. Negative contributions to the ΔS arise from losses in translational and rotational degrees of freedom that reduce the flexibility of the nucleotide−sugar and/or residues in the GFPP active site upon binding. Hence, GFPP may be using an entropic screening process to help determine the substrate from the nonsubstrate.

Large negative changes in ΔC_p are indicative of removing large amounts of protein surface area from interactions with the solvent (*43*). This, coupled with the temperature depen-

dence of the entropy and enthalpy (for binding of substrates with unfavorable entropic terms), may indicate that GFPP alters the solvent-accessible surface area and thus conformation, in response to nucleotide−sugar binding. There are no observable changes to the GFPP hydrodynamic radius or to the circular dichroism spectrum (data not shown) that would indicate a large conformational change. This, in turn, may mean that the alterations to the accessible surface area are caused by more subtle conformational changes, perhaps involving surface loops. This particular phenomenon has been seen in other nucleotide-binding proteins (*44*).

Many binding reactions involve transfer of protons to or from the complex. This often has a large effect on the binding affinity. Experiments were performed to assess whether binding involved a change in the protonation state of a titratable group (or groups) in the GFPP active site. Calorimetric analysis of GFPP-GDP-β-L-fucose binding in different buffers indicates that no protons are transferred as a result of binding (slope = 0.01 in a plot of ΔH_{app} versus ΔH_{ion} from the relation $\Delta H_{app} = n\Delta H_{cor} + \Delta H_{ioiz}$; data not shown). However, it may also be possible that net proton transfer in the active site is masked by proton transfer between a part of GFPP that is remote from the active site and the buffer. Any such alterations to the p*K* outside of the active site would compensate for changes within the active site (*42*).

GFPP is unlike many of the other nucleotide−sugar pyrophosphorylases, including primary sequence identity, quaternary structure, regulation, tissue distribution, and substrate preferences. When more of the enzyme architecture and mechanism is unraveled, it will be possible to further the understanding of fucose metabolism in diverse species. This study dissected the discrimination of GFPP for substrates and nonsubstrates as a method for characterizing the enzyme active site. The ultimate analysis of the GFPP active site will come from combining this binding analysis with the elucidation of the three-dimensional structure of GFPP complexed with substrate and inhibitor molecules. Crystallization trials are underway, but so far, the enzyme has proven recalcitrant to forming diffraction quality crystals. In the meantime, a large amount of useful information can be determined about this system using traditional enzymology.

REFERENCES

1. Becker, D. J., and Lowe, J. B. (2003) Fucose: Biosynthesis and biological function in mammals, *Glycobiology 13*, 41R−53R.
2. Walz, G., Aruffo, A., Kolanus, W., Bevilacqua, M., and Seed, B. (1990) Recognition by ELAM-1 of the sialyl-Lex determinant on myeloid and tumor cells, *Science 250*, 1132−1135.
3. Phillips, M. L., Nudelman, E., Gaeta, F. C., Perez, M., Singhal, A. K., Hakomori, S., and Paulson, J. C. (1990) ELAM-1 mediates cell adhesion by recognition of a carbohydrate ligand, sialyl-Lex, *Science 250*, 1130−1132.
4. Fenderson, B. A., Zehavi, U., and Hakomori, S. (1984) A multivalent lacto-*N*-fucopentaose III-lysyllysine conjugate decompacts preimplantation mouse embryos, while the free oligosaccharide is ineffective, *J. Exp. Med. 160*, 1591−1596.
5. Amano, J., Straehl, P., Berger, E. G., Kochibe, N., and Kobata, A. (1991) Structures of mucin-type sugar chains of the galactosyltransferase purified from human milk. Occurrence of the ABO and Lewis blood group determinants, *J. Biol. Chem. 266*, 11461−11477.
6. Yorek, M. A., and Dunlap, J. A. (2002) Effect of increased concentration of D-glucose or L-fucose on monocyte adhesion to endothelial cell monolayers and activation of nuclear factor-κB, *Metabolism 51*, 225−234.
7. Wu, B., Zhang, Y., and Wang, P. G. (2001) Identification and characterization of GDP-D-mannose 4,6-dehydratase and GDP-L-fucose snthetase in a GDP-L-fucose biosynthetic gene cluster from *Helicobacter pylori*, *Biochem. Biophys. Res. Commun. 285*, 364−371.
8. Korner, C., Linnebank, M., Koch, H. G., Harms, E., von Figura, K., and Marquardt, T. (1999) Decreased availability of GDP-L-fucose in a patient with LAD II with normal GDP-D-mannose dehydratase and FX protein activities, *J. Leukocyte Biol. 66*, 95−98.
9. Jork, R., Grecksch, G., and Matthies, H. (1986) Impairment of glycoprotein fucosylation in rat hippocampus and the consequences on memory formation, *Pharmacol. Biochem. Behav. 25*, 1137−1144.
10. Angenstein, F., Matthies, H., Jr., Staeck, S., Reymann, K. G., and Staak, S. (1992) The maintenance of hippocampal long-term potentiation is paralleled by a dopamine-dependent increase in glycoprotein fucosylation, *Neurochem. Int. 21*, 403−408.
11. Bulet, P., Hoflack, B., Porchet, M., and Verbert, A. (1984) Study of the conversion of GDP-mannose into GDP-fucose in Nereids: A biochemical marker of oocyte maturation, *Eur. J. Biochem. 144*, 255−259.
12. Park, S. H., Pastuszak, I., Drake, R., and Elbein, A. D. (1998) Purification to apparent homogeneity and properties of pig kidney L-fucose kinase, *J. Biol. Chem. 273*, 5685−5691.
13. Hinderlich, S., Berger, M., Blume, A., Chen, H., Ghaderi, D., and Bauer, C. (2002) Identification of human L-fucose kinase amino acid sequence, *Biochem. Biophys. Res. Commun. 294*, 650−654.
14. Pastuszak, I., Ketchum, C., Hermanson, G., Sjoberg, E. J., Drake, R., and Elbein, A. D. (1998) GDP-L-fucose pyrophosphorylase. Purification, cDNA cloning, and properties of the enzyme, *J. Biol. Chem. 273*, 30165−30174.
15. Zuccotti, S., Zanardi, D., Rosano, C., Sturla, L., Tonetti, M., and Bolognesi, M. (2001) Kinetic and crystallographic analyses support a sequential-ordered bi bi catalytic mechanism for *Escherichia coli* glucose-1-phosphate thymidylyltransferase, *J. Mol. Biol. 313*, 831−843.
16. Campbell, R. E., Mosimann, S. C., Tanner, M. E., and Strynadka, N. C. (2000) The structure of UDP-*N*-acetylglucosamine 2-epimerase reveals homology to phosphoglycosyl transferases, *Biochemistry 39*, 14993−15001.
17. Thoden, J. B., Ruzicka, F. J., Frey, P. A., Rayment, I., and Holden, H. M. (1997) Structural analysis of the H166G site-directed mutant of galactose-1-phosphate uridylyltransferase complexed with either UDP-glucose or UDP-galactose: Detailed description of the nucleotide sugar binding site, *Biochemistry 36*, 1212−1222.
18. Blankenfeldt, W., Kerr, I. D., Giraud, M. F., McMiken, H. J., Leonard, G., Whitfield, C., Messner, P., Graninger, M., and Naismith, J. H. (2002) Variation on a theme of SDR. dTDP-6-deoxy-L-lyxo-4-hexulose reductase (RmlD) shows a new Mg^{2+}-dependent dimerization mode, *Structure 10*, 773−786.
19. Thoden, J. B., Henderson, J. M., Fridovich-Keil, J. L., and Holden, H. M. (2002) Structural analysis of the Y299C mutant of *Escherichia coli* UDP-galactose 4-epimerase. Teaching an old dog new tricks, *J. Biol. Chem. 277*, 27528−27534.
20. Campbell, R. E., Mosimann, S. C., van De Rijn, I., Tanner, M. E., and Strynadka, N. C. (2000) The first structure of UDP-glucose dehydrogenase reveals the catalytic residues necessary for the two-fold oxidation, *Biochemistry 39*, 7012−7023.
21. Rosano, C., Bisso, A., Izzo, G., Tonetti, M., Sturla, L., De Flora, A., and Bolognesi, M. (2000) Probing the catalytic mechanism of GDP-4-keto-6-deoxy-D-mannose epimerase/reductase by kinetic and crystallographic characterization of site-specific mutants, *J. Mol. Biol. 303*, 77−91.
22. Somoza, J. R., Menon, S., Schmidt, H., Joseph-McCarthy, D., Dessen, A., Stahl, M. L., Somers, W. S., and Sullivan, F. X. (2000) Structural and kinetic analysis of *Escherichia coli* GDP-mannose 4,6-dehydratase provides insights into the enzyme's catalytic mechanism and regulation by GDP-fucose, *Structure Fold Des. 8*, 123−135.
23. Fukui, T., Kazuta, Y., Katsube, T., Tagaya, M., and Tanizawa, K. (1993) Exploring the active site in UDP-glucose pyrophosphorylase by affinity labelling and site-directed mutagenesis, *Biotechnol. Appl. Biochem. 18* (part 2), 209−216.
24. Sambrook, J., and Russell, D. (2001) *Molecular Cloning. A Laboratory Manual*, 3rd ed., Vol. 2, Cold Spring Harbor Press, Cold Spring Harbor, New York.

25. Bradford, M. M. (1976) A rapid and sensitive method for the quantitation of microgram quantities of protein utilizing the principle of protein-dye binding, *Anal. Biochem. 72*, 248−254.
26. Seley, K. L., Zhang, L., Hagos, A., and Quirk, S. (2002) "Fleximers". Design and synthesis of a new class of novel shape-modified nucleosides, *J. Org. Chem. 67*, 3365−3373.
27. Seley, K. L., Quirk, S., Salim, S., Zhang, L., and Hagos, A. (2003) Unexpected inhibition of *S*-adenosyl-L-homocysteine hydrolase by a guanosine nucleoside, *Bioorg. Med. Chem. Lett. 13*, 1985−1988.
28. Moore, C. L., Chiaramonte, M., Higgins, T., and Kuchta, R. D. (2002) Synthesis of nucleotide analogues that potently and selectively inhibit human DNA primase, *Biochemistry 41*, 14066−14075.
29. Burgess, K., and Cook, D. (2000) Syntheses of nucleoside triphosphates, *Chem. Rev. 100*, 2047−2060.
30. Segel, I. H. (1993) *Enzyme Kinetics: Behavior and Analysis of Rapid Equilibrium and Steady-State Enzyme Systems*, John Wiley and Sons, Inc., New York.
31. Freire, E., van Osdol, W. W., Mayorga, O. L., and Sanchez-Ruiz, J. M. (1990) Calorimetrically determined dynamics of complex unfolding transitions in proteins, *Annu. Rev. Biophys. Biophys. Chem. 19*, 159−188.
32. Mori, E., Hedrick, J. L., Wardrip, N. J., Mori, T., and Takasaki, S. (1998) Occurrence of reducing terminal *N*-acetylglucosamine 3-sulfate and fucosylated outer chains in acidic N-glycans of porcine zona pellucida glycoproteins, *Glycoconjate J. 15*, 447−456.
33. Hiraishi, K., Suzuki, K., Hakomori, S., and Adachi, M. (1993) Le(y) antigen expression is correlated with apoptosis (programmed cell death), *Glycobiology 3*, 381−390.
34. Tonetti, M., Sturla, L., Bisso, A., Zanardi, D., Benatti, U., and De Flora, A. (1998) The metabolism of 6-deoxyhexoses in bacterial and animal cells, *Biochimie 80*, 923−931.
35. Marques, A. R., Ferreira, P. B., Sa-Correia, I., and Fialho, A. M. (2003) Characterization of the ugpG gene encoding a UDP-glucose pyrophosphorylase from the gellan gum producer *Sphingomonas paucimobilis* ATCC 31461, *Mol. Genet. Genomics 268*, 816−824.
36. Ballicora, M. A., Iglesias, A. A., and Preiss, J. (2003) ADP-glucose pyrophosphorylase, a regulatory enzyme for bacterial glycogen synthesis, *Microbiol. Mol. Biol. Rev. 67*, 213−225, table of contents.
37. Legler, P. M., Massiah, M. A., Bessman, M. J., and Mildvan, A. S. (2000) GDP-mannose mannosyl hydrolase catalyzes nucleophilic substitution at carbon, unlike all other Nudix hydrolases, *Biochemistry 39*, 8603−8608.
38. Yurchenco, P. D., and Atkinson, P. H. (1977) Equilibration of fucosyl glycoprotein pools in HeLa cells, *Biochemistry 16*, 944−953.
39. Niittymaki, J., Mattila, P., Roos, C., Huopaniemi, L., Sjoblom, S., and Renkonen, R. (2004) Cloning and expression of murine enzymes involved in the salvage pathway of GDP-L-fucose, *Eur. J. Biochem. 271*, 78−86.
40. Quirk, S., and Do, B. T. (1997) Cloning, purification, and characterization of the *Shigella boydii* dGTP triphosphohydrolase, *J. Biol. Chem. 272*, 332−336.
41. Burton, R. E., Baker, T. A., and Sauer, R. T. (2003) Energy-dependent degradation: Linkage between ClpX-catalyzed nucleotide hydrolysis and protein−substrate processing, *Protein Sci. 12*, 893−902.
42. Forstner, M., Berger, C., and Wallimann, T. (1999) Nucleotide binding to creatine kinase: An isothermal titration microcalorimetry study, *FEBS Lett. 461*, 111−114.
43. Sturtevant, J. M. (1977) Heat capacity and entropy changes in processes involving proteins, *Proc. Natl. Acad. Sci. U.S.A. 74*, 2236−2240.
44. den Blaauwen, T., van der Wolk, J. P., van der Does, C., van Wely, K. H., and Driessen, A. J. (1999) Thermodynamics of nucleotide binding to NBS-I of the *Bacillus subtilis* preprotein translocase subunit SecA, *FEBS Lett. 458*, 145−150.

BI0503605